Journal of Sound and Vibration (1998) **209**(4), 571–592

ON MODELLING VARIABLE STRUCTURE DYNAMICS OF HYBRID PARAMETER MULTIPLE BODY SYSTEMS

A. A. Barhorst

Mechanical Engineering, *Texas Tech University*, *Lubbock*, *TX* 79409-1021, *U.S.A.*

(*Received* 11 *December* 1996, *and in final form* 30 *June* 1997)

Recently a methodology for closed-form modelling of non-holonomic hybrid parameter multiple body systems (HPMBS) was presented. The tool provides a means to model non-holonomic HPMBS with sets of minimal closed-form hybrid differential equations; these equations are minimal in the sense that there are no Lagrange multiplier equations required. Also provided by the method is a means to generate closed-form models of the momentum change imparted on a HPMBS when the system undergoes impulsive loads or configuration space changes. In this paper, these techniques will be merged to form an algorithm for modelling HPMBS under the influence of changes in the configuration space due to the variable presence of, or lack of, constraints. It should be noted that restitution coefficients are not needed to describe momentum transferred within the system when the configuration changes. Included in this work is the explicit minimal closed-form model of a flexible two-link planar manipulator interacting with a work-piece and the numerical simulation of this system under various conditions. The process of modelling this system will elucidate the algorithm which is applicable to higher order systems.

1. INTRODUCTION

Modelling tools applicable to hybrid parameter multiple body systems (HPMBS) are in an evolutionary stage. In many instances, tools from rigid multibody systems have been adapted to model flexible systems [1, 2]. In other cases distributed parameter modelling techniques have been applied [3–5]. There is work in the numerical aspects of the solution of the modelling equations [6–8], in the modelling of configuration space variability (variable structure) [9–23], and in the generation and elucidation of the best ways to incorporate constraints [24–34]. An in-depth analysis of the merits of the cross-section of techniques is not provided in this paper, however these citations are provided so that the breadth of the work in multiple body system modelling is recognized.

Another approach, not represented above, applicable to the modelling and analysis of HPMBS has been recently presented [35, 36]. In this technique, minimal explicit equations of motion can be generated for arbitrarily complex non-holonomic HPMBS. These equations are minimal in the sense that no Lagrange multipliers are needed. Equations for modelling generalized momentum transfer in HPMBS are also provided.

In this paper, the work discussed immediately above is merged into a modelling algorithm developed in an effort to address technical issues that still exist in the area of non-holonomic HPMBS analysis. The unresolved issue addressed herein is the need for a technique that generates closed-form minimal equations of motions for HPMBS that can be readily implemented and works across variable structure systems. This effort will show it is possible to model the full motion regime dynamics (including contact and impact) of

0022–460X/98/040571 + 22 $25.00/0/sv971277

non-holonomic HPMBS in a concise, accurate, explicit, and minimal manner; it will also show that experimental restitution coefficients are not imminently required. The algorithm is developed via a modelling example and numerical results. This example is simple enough to be tractable by hand yet complicated to a degree that shows the applicability of the algorithm to increasingly more complicated systems.

The paper will proceed by providing the closed-form minimal model of a two-link planar elastic robot interacting with a work-piece; this includes equations for the free-flight motion, the contact/impact motion, and the constrained motion. Presented next is the outline of a procedure to provide for numerical simulations. Then, finally, numerical results are presented with animation snapshots.

This particular model encompasses many real-world applications such as tree-structured spacecraft and robots, and closed-link mechanisms such as the four-bar mechanisms in automobile suspensions. The example also encompasses the regime that exists when a machine is of variable structure (e.g., a robot) and transitions from a tree-structure to a closed-loop structure and vice-versa.

2. ALGORITHM BY EXAMPLE

In this section an algorithm useful for modelling HPMBS experiencing variable configuration space dimensionality will be presented. First the closed-form model of the system will be presented, then the outline and results of numerical analysis will follow. The theory used to developed the enclosed algorithm can be found elsewhere [35, 36]. The notation is borrowed from this previous work; an explanation of the terms will be provided when needed.

The system is shown in Figure 1 in an unconstrained configuration and in Figure 2 in its constrained configuration. The domain of each beam is one-dimensional, the independent co-ordinates are x_{11} and x_{21} measured from the root of beam B_1 and B_2, respectively, along the undeformed neutral axis of each beam. The "special" point of beam B_1 is labelled b_{o1} and b_{o2} for beam B_2. The co-ordinate frames, denoted with B_1 and B_2, are attached as shown in Figure 1. The Newtonian frame is denoted with $\mathcal{N}$. At the root of each beam there is a massless hub to which torques M_1 and M_2 are applied to hubs of B_1 and B_2. The angular position of frames B_1 and B_2 are q_1 and q_5. Beam deflection is

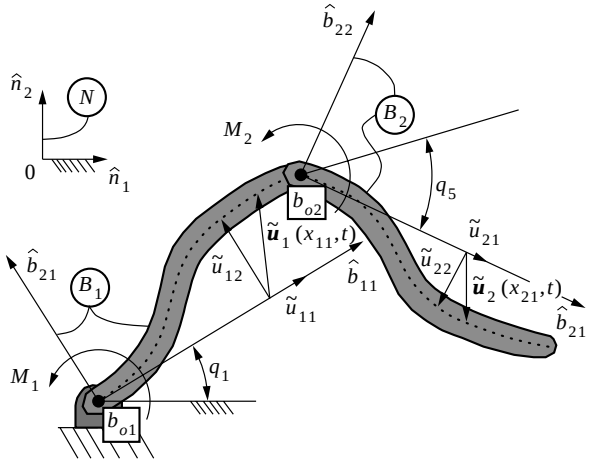

Figure 1. Two link flexible manipulator.

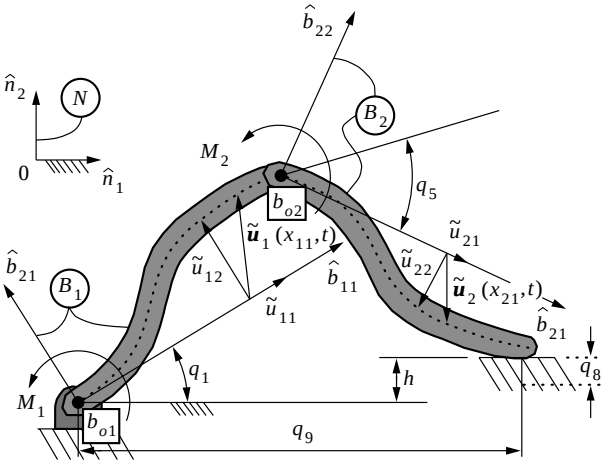

Figure 2. Constrained two link flexible manipulator.

measured with $\tilde{u}_{11}(x_{11}, t)\hat{b}_{11}$ and $\tilde{u}_{21}(x_{2i}, t)\hat{b}_{21}$ (elongation), $\tilde{u}_{12}(x_{11}, t)\hat{b}_{12}$ and $\tilde{u}_{22}(x_{21}, t)\hat{b}_{22}$ (flexure) as shown in Figure 1. The beams have mass per unit length ρ, total lengths are L_1 and L_2, cross-sectional area A, area moment of inertia I, and Young's modulus E. Additional co-ordinates, shown in Figure 2, will be discussed during the constrained system modelling stage.

2.1. FREE-FLIGHT

In this section the equations of motion for the machine in its unconstrained mode will be developed. First we start with the co-ordinate selection and kinematics, then end with the equations of motion in first order form for the free-flight.

The generalized and pseudo-generalized (denoted with primes) co-ordinates and speeds are chosen as follows:

$$s_1 = \dot{q}_1, \qquad q_4' = \frac{\partial \tilde{u}_{12}(L_1, t)}{\partial x_{11}}, \qquad s_4' = \dot{q}_4' = \frac{\partial^2 \tilde{u}_{12}(L_1, t)}{\partial x_{11}\, \partial t}, \tag{1}$$

$$s_5 = \dot{q}_5, \qquad q_2' = \tilde{u}_{11}(L_1, t), \qquad s_2' = \dot{q}_2' = \frac{\partial \tilde{u}_{11}(L_1, t)}{\partial t}, \tag{2}$$

$$q_3' = \tilde{u}_{12}(L_1, t), \qquad s_3' = \dot{q}_3' = \frac{\partial \tilde{u}_{12}(L_1, t)}{\partial t}. \tag{3}$$

The speeds are used to parameterize the configuration space of the system. The d.o.f. are infinite in this system due to the distributed parameter nature of the beams, however the discrete d.o.f. are two, one for each angular rate of the beams. The pseudo-speeds are chosen at the interconnections of the bodies to describe how the kinematic constraints must be enforced. The details of the variational basis for the choice of the pseudo-speeds can be found in the work mentioned above. In the equations below, note how the pseudo-co-ordinates and speeds are used as if they are regular generalized co-ordinates and speeds.

The angular velocity of frame B_1 and B_2 can be written as

$$^{N}\boldsymbol{\omega}^{B_1} = s_1 \hat{b}_{13} \quad \text{and} \quad ^{N}\boldsymbol{\omega}^{B_2} = (s_1 + s_4' + s_5)\hat{b}_{13}. \tag{4}$$

The absolute velocity of the point b_{o1} and b_{o2} are also required. Since the system is rotating about b_{o1}:

$$ {}^{o}_{\mathcal{N}}\mathbf{v}^{b_{o1}} = 0 \quad \text{and} \quad {}^{o}_{\mathcal{N}}\mathbf{v}^{b_{o2}} = (s_2' - s_1 q_3')\hat{b}_{11} + (s_3' + s_1(L_1 + q_2'))\hat{b}_{12}. \tag{5} $$

The absolute acceleration of the differential beam element dm_1 for beam B_1 can be written as

$$ {}^{o}_{\mathcal{N}}\mathbf{a}^{\mathrm{d}m_1} = \left(\frac{\partial^2 \tilde{u}_{11}}{\partial t^2} - \dot{s}_1 \tilde{u}_{12} - 2s_1 \frac{\partial \tilde{u}_{12}}{\partial t} - (x_{11} + \tilde{u}_{11})s_1^2\right)\hat{b}_{11} $$

$$ + \left(\frac{\partial^2 \tilde{u}_{12}}{\partial t^2} + (x_{11} + \tilde{u}_{11})\dot{s}_1 + 2s_1 \frac{\partial \tilde{u}_{11}}{\partial t} - \tilde{u}_{12}s_1^2\right)\hat{b}_{12}. \tag{6} $$

The absolute acceleration of the differential beam element $\mathrm{d}m_2$ for beam B_2 can be written as

$$ {}^{o}_{\mathcal{N}}\mathbf{a}^{\mathrm{d}m_2} = (\dot{s}_2' - \dot{s}_1 q_3' - 2s_1 s_3' - (L_1 + q_2')s_1^2)\hat{b}_{11} + (\dot{s}_3' + (L_1 + q_2')\dot{s}_1 + 2s_1 s_2' - q_3' s_1^2)\hat{b}_{12} $$

$$ + \left(\frac{\partial^2 \tilde{u}_{21}}{\partial t^2} - (\dot{s}_1 + \dot{s}_4' + \dot{s}_5)\tilde{u}_{22} - 2(s_1 + s_4' + s_5)\frac{\partial \tilde{u}_{22}}{\partial t} - (x_{21} + \tilde{u}_{21})(s_1 + s_4' + s_5)^2\right)\hat{b}_{21} $$

$$ + \left(\frac{\partial^2 \tilde{u}_{22}}{\partial t^2} + (x_{21} + \tilde{u}_{21})(\dot{s}_1 + \dot{s}_4' + \dot{s}_5) + 2(s_1 + s_4' + s_5)\frac{\partial \tilde{u}_{21}}{\partial t} - \tilde{u}_{22}(s_1 + s_4' + s_5)^2\right)\hat{b}_{22}. \tag{7} $$

The strain energy density functions for the beams B_i $(i = 1, 2)$ are (assuming large deflections)

$$ \bar{V}_i = \frac{1}{2}EA\left(\frac{\partial \tilde{u}_{i1}}{\partial x_{i1}} + \frac{1}{2}\left(\frac{\partial \tilde{u}_{i2}}{\partial x_{i1}}\right)^2\right)^2 + \frac{1}{2}EI\left(\frac{\partial^2 \tilde{u}_{i2}}{\partial x_{i1}^2}\right)^2. \tag{8} $$

The torques applied to the massless hubs are

$$ \mathbf{T}_1 = M_1 \hat{b}_{13} \quad \text{and} \quad \mathbf{T}_2 = M_2 \hat{b}_{23} \tag{9} $$

on B_1 and B_2, respectively. The weight of the system is ignored assuming the system moves in a plane perpendicular to local gravity.

The methodology also requires the calculations of the "preferred directions" for the variations (pseudo and ordinary); these are tabulated in Table 1 using equations (4) and (5): the equations of motion can now be written down.

2.1.1. *ODE's*

The ordinary differential equations modelling the angular positions are

$$ 0 = \frac{\partial^{o}_{\mathcal{A}}\mathbf{v}^{b_{o1}}}{\partial s_1} \cdot [\mathbf{F}_{B_1} - \mathbf{I}_{B_1}] + \frac{\partial^{\mathcal{N}}\boldsymbol{\omega}^{B_1}}{\partial s_1} \cdot [\mathbf{T}_{B_1} - \mathbf{J}_{B_1}] + \frac{\partial^{o}_{\mathcal{A}}\mathbf{v}^{b_{o2}}}{\partial s_1} \cdot [\mathbf{F}_{B_2} - \mathbf{I}_{B_2}] $$

$$ + \frac{\partial^{\mathcal{N}}\boldsymbol{\omega}^{B_2}}{\partial s_1} \cdot [\mathbf{T}_{B_2} - \mathbf{J}_{B_2}] \tag{10} $$

for s_1, and

$$0 = \frac{\partial^o_{\mathcal{N}} \mathbf{v}^{b_{o1}}}{\partial s_5} \cdot [\mathbf{F}_{B_1} - \mathbf{I}_{B_2}] + \frac{\partial^{\mathcal{N}} \boldsymbol{\omega}^{B_1}}{\partial s_5} \cdot [\mathbf{T}_{B_1} - \mathbf{J}_{B_1}] + \frac{\partial^o_{\mathcal{N}} \mathbf{v}^{b_{o2}}}{\partial s_5} \cdot [\mathbf{F}_{B_2} - \mathbf{I}_{B_2}]$$
$$+ \frac{\partial^{\mathcal{N}} \boldsymbol{\omega}^{B_2}}{\partial s_5} \cdot [\mathbf{T}_{B_2} - \mathbf{J}_{B_2}] \tag{11}$$

for s_5. The formula for forces and torques (applied and inertia) were defined in the previous work. The applied loads were described above.

Performing the required vector cross and dot products implied in equations (10) and (11) and rearranging the equations gives

$$\begin{bmatrix} I_{11} & I_{12} \\ I_{21} & I_{22} \end{bmatrix} \begin{Bmatrix} \dot{s}_1 \\ \dot{s}_5 \end{Bmatrix} = \begin{Bmatrix} f_1 \\ f_2 \end{Bmatrix}. \tag{12}$$

The elements of the inertia matrix and the force vector are defined as

$$I_{11} = \int_0^{L_1} \rho[(x_{11} + \tilde{u}_{11})^2 + \tilde{u}_{12}^2]\, \mathrm{d}x_{11} + [q_3'^2 + (L_1 + q_2')^2] \int_0^{L_2} \rho\, \mathrm{d}x_{21}$$
$$+ q_3' \int_0^{L_2} \rho \tilde{u}_{22}\, \mathrm{d}x_{21} (\hat{b}_{11} \cdot \hat{b}_{21}) - q_3' \int_0^{L_2} \rho (x_{21} + \tilde{u}_{21})\, \mathrm{d}x_{21} (\hat{b}_{11} \cdot \hat{b}_{22})$$
$$- (L_1 + q_2') \int_0^{L_2} \rho \tilde{u}_{22}\, \mathrm{d}x_{21} (\hat{b}_{12} \cdot \hat{b}_{21}) + (L_1 + q_2') \int_0^{L_2} \rho (x_{21} + \tilde{u}_{21})\, \mathrm{d}x_{21} (\hat{b}_{12} \cdot \hat{b}_{22})$$
$$- q_3' \int_0^{L_2} \rho \tilde{u}_{22}\, \mathrm{d}x_{21} (\hat{b}_{22} \times \hat{b}_{11}) \cdot \hat{b}_{13} - q_3' \int_0^{L_2} \rho (x_{21} + \tilde{u}_{21})\, \mathrm{d}x_{21} (\hat{b}_{21} \times \hat{b}_{11}) \cdot \hat{b}_{13}$$
$$+ (L_1 + q_2') \int_0^{L_2} \rho \tilde{u}_{22}\, \mathrm{d}x_{21} (\hat{b}_{22} \times \hat{b}_{12}) \cdot \hat{b}_{13}$$
$$+ (L_1 + q_2') \int_0^{L_2} \rho (x_{21} + \tilde{u}_{21})\, \mathrm{d}x_{21} (\hat{b}_{21} \times \hat{b}_{12}) \cdot \hat{b}_{13} + \int_0^{L_2} \rho[(x_{21} + \tilde{u}_{21})^2 + \tilde{u}_{22}^2]\, \mathrm{d}x_{21},$$

TABLE 1

Partial velocities

	${}^o_{\mathcal{N}}\mathbf{v}^{b_{o1}}$	${}^o_{\mathcal{N}}\mathbf{v}^{b_{o2}}$	${}^{\mathcal{N}}\boldsymbol{\omega}^{B_1}$	${}^{\mathcal{N}}\boldsymbol{\omega}^{B_2}$
$\frac{\partial}{\partial s_1}$	0	$-g_3' \hat{b}_{11} + (L_1 + g_2') \hat{b}_{12}$	$\hat{b}_{13}$	$\hat{b}_{13}$
$\frac{\partial}{\partial s_2'}$	0	$\hat{b}_{11}$	0	0
$\frac{\partial}{\partial s_3'}$	0	$\hat{b}_{12}$	0	0
$\frac{\partial}{\partial s_4'}$	0	0	0	$\hat{b}_{13}$
$\frac{\partial}{\partial s_5}$	0	0	0	$\hat{b}_{13}$

$$I_{12} = q_3' \int_0^{L_2} \rho \tilde{u}_{22}\, \mathrm{d}x_{21}(\hat{b}_{11} \cdot \hat{b}_{21}) - q_3' \int_0^{L_2} \rho(x_{21} + \tilde{u}_{21})\, \mathrm{d}x_{21}(\hat{b}_{11} \cdot \hat{b}_{22})$$

$$- (L_1 + q_2') \int_0^{L_2} \rho \tilde{u}_{22}\, \mathrm{d}x_{21}(\hat{b}_{12} \cdot \hat{b}_{21}) + (L_1 + q_2') \int_0^{L_2} \rho(x_{21} + \tilde{u}_{21})\, \mathrm{d}x_{21}(\hat{b}_{12} \cdot \hat{b}_{22})$$

$$+ \int_0^{L_2} \rho[(x_{21} + \tilde{u}_{21})^2 + \tilde{u}_{22}^2]\, \mathrm{d}x_{21},$$

$$I_{21} = -q_3' \int_0^{L_2} \rho \tilde{u}_{22}\, \mathrm{d}x_{21}(\hat{b}_{22} \times \hat{b}_{11}) \cdot \hat{b}_{13} - q_3' \int_0^{L_2} \rho(x_{21} + \tilde{u}_{21})\, \mathrm{d}x_{21}(\hat{b}_{21} \times \hat{b}_{11}) \cdot \hat{b}_{13}$$

$$+ (L_1 + q_2') \int_0^{L_2} \rho \tilde{u}_{22}\, \mathrm{d}x_{21}(\hat{b}_{22} \times \hat{b}_{12}) \cdot \hat{b}_{13}$$

$$+ (L_1 + q_2') \int_0^{L_2} \rho(x_{21} + \tilde{u}_{21})\, \mathrm{d}x_{21}(\hat{b}_{21} \times \hat{b}_{12}) \cdot \hat{b}_{13} + \int_0^{L_2} \rho[(x_{21} + \tilde{u}_{21})^2 + \tilde{u}_{22}^2]\, \mathrm{d}x_{21}$$

and

$$I_{22} = \int_0^{L_2} \rho[(x_{21} + \tilde{u}_{21})^2 + \tilde{u}_{22}^2]\, \mathrm{d}x_{21}.$$

The term I_{11} can be reduced further if the properties of the vector-scalar triple product are used. The right-hand side terms of equation (12) can be written as

$$f_1 = M_1 - \int_0^{L_1} \rho \Bigg\{ \frac{\partial^2 \tilde{u}_{12}}{\partial t^2}(x_{11} + \tilde{u}_{11}) + 2s_1 \frac{\partial \tilde{u}_{11}}{\partial t}(x_{11} + \tilde{u}_{11}) - s_1^2 \tilde{u}_{12}(x_{11} + \tilde{u}_{11}) - \tilde{u}_{12} \frac{\partial^2 \tilde{u}_{11}}{\partial t^2}$$

$$+ 2s_1 \frac{\partial \tilde{u}_{12}}{\partial t} \tilde{u}_{12} + s_1^2 \tilde{u}_{12}(x_{11} + \tilde{u}_{11}) \Bigg\} \mathrm{d}x_{11} + q_3' \int_0^{L_2} \rho \Bigg\{ \Bigg[\frac{\partial^2 \tilde{u}_{21}}{\partial t^2} - \dot{s}_4' \tilde{u}_{22}$$

$$- 2(s_1 + s_4' + s_5) \frac{\partial \tilde{u}_{22}}{\partial t} - (s_1 + s_4' + s_5)^2 (x_{21} + \tilde{u}_{21}) \Bigg] (\hat{b}_{11} \cdot \hat{b}_{21}) + \Bigg[\frac{\partial^2 \tilde{u}_{22}}{\partial t^2} + \dot{s}_4'(x_{21} + \tilde{u}_{21})$$

$$+ 2(s_1 + s_4' + s_5) \frac{\partial \tilde{u}_{21}}{\partial t} - (s_1 + s_4' + s_5)^2 \tilde{u}_{22} \Bigg] (\hat{b}_{11} \cdot \hat{b}_{22}) + \dot{s}_2' - 2s_1 s_3' - s_1^2 (L_1 + q_2') \Bigg\} \mathrm{d}x_{21}$$

$$- (L_1 + q_2') \int_0^{L_2} \rho \Bigg\{ \Bigg[\frac{\partial^2 \tilde{u}_{21}}{\partial t^2} - \dot{s}_4' \tilde{u}_{22} - 2(s_1 + s_4' + s_5) \frac{\partial \tilde{u}_{22}}{\partial t}$$

$$- (s_1 + s_4' + s_5)^2 (x_{21} + \tilde{u}_{21}) \Bigg] (\hat{b}_{12} \cdot \hat{b}_{21}) + \Bigg[\frac{\partial^2 \tilde{u}_{22}}{\partial t^2} + \dot{s}_4'(x_{21} + \tilde{u}_{21})$$

$$+ 2(s_1 + s_4' + s_5)\frac{\partial \tilde{u}_{21}}{\partial t} - (s_1 + s_4' + s_5)^2\tilde{u}_{22}\Big](\hat{b}_{12}\cdot\hat{b}_{22}) + \dot{s}_3' + 2s_1s_2' - s_1^2q_3'\Big\}\,\mathrm{d}x_{21} + M_2$$

$$- \int_0^{L_2} \rho(x_{21} + \tilde{u}_{21})\,\mathrm{d}x_{21}[\dot{s}_2' - 2s_1s_3' - s_1^2(L_1 + q_2')](\hat{b}_{21}\times\hat{b}_{11})\cdot\hat{b}_{13}$$

$$- \int_0^{L_2} \rho\tilde{u}_{22}\,\mathrm{d}x_{21}[\dot{s}_2' - 2s_1s_3' - s_1^2(L_1 + q_2')](\hat{b}_{22}\times\hat{b}_{11})\cdot\hat{b}_{13}$$

$$- \int_0^{L_2} \rho(x_{21} + \tilde{u}_{21})\,\mathrm{d}x_{21}[\dot{s}_3' + 2s_1s_2' - s_1^2q_3'](\hat{b}_{21}\times\hat{b}_{12})\cdot\hat{b}_{13}$$

$$- \int_0^{L_2} \rho\tilde{u}_{22}\,\mathrm{d}x_{21}[\dot{s}_3' + 2s_1s_2' - s_1^2q_3'](\hat{b}_{22}\times\hat{b}_{12})\cdot\hat{b}_{13}$$

$$- \int_0^{L_2} \rho(x_{21} + \tilde{u}_{21})\Big[\frac{\partial^2\tilde{u}_{22}}{\partial t^2} + \dot{s}_4'(x_{21} + \tilde{u}_{21}) + 2(s_1 + s_4' + s_5)\frac{\partial\tilde{u}_{21}}{\partial t}$$

$$- (s_1 + s_4' + s_5)^2\tilde{u}_{22}\Big]\mathrm{d}x_{21} + \int_0^{L_2}\rho\tilde{u}_{22}\Big[\frac{\partial^2\tilde{u}_{21}}{\partial t^2} - \dot{s}_4'\tilde{u}_{22} - 2(s_1 + s_4' + s_5)\frac{\partial\tilde{u}_{22}}{\partial t}$$

$$- (s_1 + s_4' + s_5)^2(x_{21} + \tilde{u}_{21})\Big]\mathrm{d}x_{21}$$

and

$$f_2 = M_2 - \int_0^{L_2} \rho(x_{21} + \tilde{u}_{21})\,\mathrm{d}x_{21}[\dot{s}_2' - 2s_1s_3' - s_1^2(L_1 + q_2')](\hat{b}_{21}\times\hat{b}_{11})\cdot\hat{b}_{13}$$

$$- \int_0^{L_1} \rho\tilde{u}_{22}\,\mathrm{d}x_{21}[\dot{s}_2' - 2s_1s_3' - s_1^2(L_1 + q_2')](\hat{b}_{22}\times\hat{b}_{11})\cdot\hat{b}_{13}$$

$$- \int_0^{L_2} \rho(x_{21} + \tilde{u}_{21})\,\mathrm{d}x_{21}[\dot{s}_3' + 2s_1s_2' - s_1^2q_3'](\hat{b}_{21}\times\hat{b}_{12})\cdot\hat{b}_{13}$$

$$- \int_0^{L_2} \rho\tilde{u}_{22}\,\mathrm{d}x_{21}[\dot{s}_3' + 2s_1s_2' - s_1^2q_3'](\hat{b}_{22}\times\hat{b}_{12})\cdot\hat{b}_{13} - \int_0^{L_2}\rho(x_{21} + \tilde{u}_{21})$$

$$\times\Big[\frac{\partial^2\tilde{u}_{22}}{\partial t^2} + \dot{s}_4'(x_{21} + \tilde{u}_{21}) + 2(s_1 + s_4' + s_5)\frac{\partial\tilde{u}_{21}}{\partial t} - (s_1 + s_4' + s_5)^2\tilde{u}_{22}\Big]\mathrm{d}x_{21}$$

$$+ \int_0^{L_2}\rho\tilde{u}_{22}\Big[\frac{\partial^2\tilde{u}_{21}}{\partial t^2} - \dot{s}_4'\tilde{u}_{22} - 2(s_1 + s_4' + s_5)\frac{\partial\tilde{u}_{22}}{\partial t} - (s_1 + s_4' + s_5)^2(x_{21} + \tilde{u}_{21})\Big]\mathrm{d}x_{21}.$$

2.1.2. *PDE;s and B.C's*

The formulas for the field equations modelling elongation and deflection can be written as

$$0 = \frac{\partial}{\partial x_{11}}\left(\frac{\partial \overline{V}_1}{\partial \tilde{u}_{11,1}}\right) - \rho^o_{\mathcal{M}} \mathbf{a}^{\mathrm{d}m_1} \cdot \hat{b}_{11} \tag{13}$$

for elongation and

$$0 = \frac{\partial}{\partial x_{11}}\left(\frac{\partial \overline{V}_1}{\partial \tilde{u}_{12,2}}\right) - \frac{\partial^2}{\partial x_{11}^2}\left(\frac{\partial \overline{V}_1}{\partial \tilde{u}_{12,11}}\right) - \rho^o_{\mathcal{M}} \mathbf{a}^{\mathrm{d}m_1} \cdot \hat{b}_{12} \tag{14}$$

for deflection. The boundary conditions can be written as:

$$\frac{\partial \overline{V}_1}{\partial \tilde{u}_{11,1}} = g'_{11}, \qquad \frac{\partial \overline{V}_1}{\partial \tilde{u}_{12,1}} - \frac{\partial}{\partial x_{11}}\left(\frac{\partial \overline{V}_1}{\partial \tilde{u}_{12,11}}\right) = g'_{12}, \qquad \frac{\partial \overline{V}_1}{\partial \tilde{u}_{12,11}} = k'_{12} \tag{15–17}$$

at $x_{11} = L_1$, and

$$\tilde{u}_{11} = \tilde{u}_{12} = \tilde{u}_{12,1} = 0 \tag{18}$$

at $x_{11} = 0$. The terms on the right-hand sides of the boundary conditions are defined as

$$g'_{11} = \frac{\partial^o_{\mathcal{M}} \mathbf{v}^{b_{o1}}}{\partial s'_2} \cdot [\mathbf{F}_{B_1} - \mathbf{I}_{B_1}] + \frac{\partial^{\mathcal{M}} \boldsymbol{\omega}^{B_1}}{\partial s'_2} \cdot [\mathbf{T}_{B_1} - \mathbf{J}_{B_1}] + \frac{\partial^o_{\mathcal{M}} \mathbf{v}^{b_{o2}}}{\partial s'_2} \cdot [\mathbf{F}_{B_2} - \mathbf{I}_{B_2}] + \frac{\partial^{\mathcal{M}} \boldsymbol{\omega}^{B_2}}{\partial s'_2} \cdot [\mathbf{T}_{B_2} - \mathbf{J}_{B_2}],$$

$$g'_{12} = \frac{\partial^o_{\mathcal{M}} \mathbf{v}^{b_{o1}}}{\partial s'_3} \cdot [\mathbf{F}_{B_1} - \mathbf{I}_{B_1}] + \frac{\partial^{\mathcal{M}} \boldsymbol{\omega}^{B_1}}{\partial s'_3} \cdot [\mathbf{T}_{B_1} - \mathbf{J}_{B_1}] + \frac{\partial^o_{\mathcal{M}} \mathbf{v}^{b_{o2}}}{\partial s'_3} \cdot [\mathbf{F}_{B_2} - \mathbf{I}_{B_2}] + \frac{\partial^{\mathcal{M}} \boldsymbol{\omega}^{B_2}}{\partial s'_3} \cdot [\mathbf{T}_{B_2} - \mathbf{J}_{B_2}]$$

and

$$k'_{12} = \frac{\partial^o_{\mathcal{M}} \mathbf{v}^{b_{b1}}}{\partial s'_4} \cdot [\mathbf{F}_{B_1} - \mathbf{I}_{B_1}] + \frac{\partial^{\mathcal{M}} \boldsymbol{\omega}^{B_1}}{\partial s'_4} \cdot [\mathbf{T}_{B_1} - \mathbf{J}_{B_1}] + \frac{\partial^o_{\mathcal{M}} \mathbf{v}^{b_{o2}}}{\partial s'_4} \cdot [\mathbf{F}_{B_2} - \mathbf{I}_{B_2}] + \frac{\partial^{\mathcal{M}} \boldsymbol{\omega}^{B_2}}{\partial s'_4} \cdot [\mathbf{T}_{B_2} - \mathbf{J}_{B_2}].$$

These last three expressions can be seen as the means that allow the pseudo-speeds to be utilized to calculate forces of constraint; in this case forces and torques on the boundary.

The field equations for the second member (B_2) are

$$0 = \frac{\partial}{\partial x_{21}}\left(\frac{\partial \overline{V}_2}{\partial \tilde{u}_{21,1}}\right) - \rho^o_{\mathcal{M}} \mathbf{a}^{\mathrm{d}m_2} \cdot \hat{b}_{21} \tag{19}$$

for elongation and

$$0 = \frac{\partial}{\partial x_{21}}\left(\frac{\partial \overline{V}_2}{\partial \tilde{u}_{22,1}}\right) - \frac{\partial^2}{\partial x_{21}^2}\left(\frac{\partial \overline{V}_2}{\partial \tilde{u}_{22,11}}\right) - \rho^o_{\mathcal{M}} \mathbf{a}^{\mathrm{d}m_2} \cdot \hat{b}_{22} \tag{20}$$

for deflection. The boundary conditions are

$$\frac{\partial \bar{V}_2}{\partial u_{21,1}} = 0, \qquad \frac{\partial \bar{V}_2}{\partial \tilde{u}_{22,1}} - \frac{\partial}{\partial x_{11}}\left(\frac{\partial \bar{V}_2}{\partial \tilde{u}_{22,11}}\right) = 0, \qquad \frac{\partial \bar{V}_2}{\partial \tilde{u}_{22,11}} = 0 \tag{21–23}$$

at $x_{21} = L_2$, and

$$\tilde{u}_{21} = \tilde{u}_{22} = \tilde{u}_{22,1} = 0 \tag{24}$$

at $x_{21} = 0$.

Performing the required differentiation results in

$$0 = \frac{\partial}{\partial x_{11}}\left[EA\left(\frac{\partial \tilde{u}_{11}}{\partial x_{11}} + \tfrac{1}{2}\left(\frac{\partial \tilde{u}_{12}}{\partial x_{11}}\right)^2\right)\right] - \rho_B\left(\frac{\partial^2 \tilde{u}_{11}}{\partial t^2} - \dot{s}_1 \tilde{u}_{12} - 2s_1 \frac{\partial \tilde{u}_{12}}{\partial t} - (x_{11} + \tilde{u}_{11})s_1^2\right) \tag{25}$$

and

$$0 = \frac{\partial}{\partial x_{11}}\left[EA\left(\frac{\partial \tilde{u}_{11}}{\partial x_{11}} + \tfrac{1}{2}\left(\frac{\partial \tilde{u}_{12}}{\partial x_{11}}\right)^2\right)\frac{\partial \tilde{u}_{12}}{\partial x_{11}}\right] - \frac{\partial^2}{\partial x_{11}^2}\left(EI\frac{\partial^2 \tilde{u}_{12}}{\partial x_{11}^2}\right)$$

$$- \rho\left(\frac{\partial^2 \tilde{u}_{12}}{\partial t^2} + 2s_1 \frac{\partial \tilde{u}_{12}}{\partial t} + (x_{11} + \tilde{u}_{11})\dot{s}_1 - \tilde{u}_{12}s_1^2\right), \tag{26}$$

replacing equations (13) and (14), respectively. Equation (15) is replaced with

$$EA\left(\frac{\partial \tilde{u}_{11}}{\partial x_{11}} + \tfrac{1}{2}\left(\frac{\partial \tilde{u}_{12}}{\partial x_{11}}\right)^2\right) = -\int_0^{L_2} \rho \, \mathrm{d}x_{21}[\dot{s}_2' - \dot{s}_1 q_3' - 2s_1 s_3' - s_1^2(L_1 + q_2')]$$

$$- \int_0^{L_2} \rho\left[\frac{\partial^2 \tilde{u}_{21}}{\partial t^2} - (\dot{s}_1 + \dot{s}_4' + \dot{s}_5)\tilde{u}_{22} - 2(s_1 + s_4' + s_5)\frac{\partial \tilde{u}_{22}}{\partial t}\right.$$

$$\left. - (s_1 + s_4' + s_5)^2(x_{21} + \tilde{u}_{21})\right](\hat{b}_{11} \cdot \hat{b}_{21}) \, \mathrm{d}x_{21}$$

$$- \int_0^{L_2} \rho\left[\frac{\partial^2 \tilde{u}_{22}}{\partial t^2} + (\dot{s}_1 + \dot{s}_4' + \dot{s}_5)(x_{21} + \tilde{u}_{21}) + 2(s_1 + s_4' + s_5)\frac{\partial \tilde{u}_{21}}{\partial t}\right.$$

$$\left. - (s_1 + s_4' + s_5)^2 \tilde{u}_{22}\right](\hat{b}_{11} \cdot \hat{b}_{22}) \, \mathrm{d}x_{21}. \tag{27}$$

Equation (16) is replaced with

$$EA\left(\frac{\partial \tilde{u}_{11}}{\partial x_{11}} + \frac{1}{2}\left(\frac{\partial \tilde{u}_{12}}{\partial x_{11}}\right)^2\right)\frac{\partial \tilde{u}_{12}}{\partial x_{11}} - \frac{\partial}{\partial x_{11}}\left(EI\frac{\partial^2 \tilde{u}_{12}}{\partial x_{11}^2}\right)$$

$$= -\int_0^{L_2} \rho \, \mathrm{d}x_{21}[\dot{s}_3' + \dot{s}_1(L_1 + q_2') + 2s_1 s_2' - s_1^2 q_3']$$

$$- \int_0^{L_2} \rho\left[\frac{\partial^2 \tilde{u}_{21}}{\partial t^2} - (\dot{s}_1 + \dot{s}_4' + \dot{s}_5)\tilde{u}_{22} - 2(s_1 + s_4' + s_5)\frac{\partial \tilde{u}_{22}}{\partial t}\right.$$

$$\left. - (s_1 + s_4' + s_5)^2(x_{21} + \tilde{u}_{21})\right](\hat{b}_{12} \cdot \hat{b}_{21}) \, \mathrm{d}x_{21}$$

$$- \int_0^{L_2} \rho\left[\frac{\partial^2 \tilde{u}_{22}}{\partial t^2} + (\dot{s}_1 + \dot{s}_4' + \dot{s}_5)(x_{21} + \tilde{u}_{21})\right.$$

$$\left. + 2(s_1 + s_4' + s_5)\frac{\partial \tilde{u}_{21}}{\partial t} - (s_1 + s_4' + s_5)^2 \tilde{u}_{22}\right](\hat{b}_{12} \cdot \hat{b}_{22}) \, \mathrm{d}x_{21}. \tag{28}$$

Equation (17) is replaced by

$$EI\frac{\partial^2 \tilde{u}_{12}}{\partial x_{11}^2} = M_2 - \int_0^{L_2} \rho(x_{21} + \tilde{u}_{21})[\dot{s}_2' - \dot{s}_1 q_3' - 2s_1 s_3' - s_1^2(L_1 + q_2')](\hat{b}_{21} \times \hat{b}_{11}) \cdot \hat{b}_{13} \, \mathrm{d}x_{21}$$

$$- \int_0^{L_2} \rho \tilde{u}_{22}[\dot{s}_2' - \dot{s}_1 q_3' - 2s_1 s_3' - s_1^2(L_1 + q_2')](\hat{b}_{22} \times \hat{b}_{11}) \cdot \hat{b}_{13} \, \mathrm{d}x_{21}$$

$$- \int_0^{L_2} \rho(x_{21} + \tilde{u}_{21})[\dot{s}_3' + \dot{s}_1(L_1 + q_2') + 2s_1 s_2' - s_1^2 q_3'](\hat{b}_{21} \times \hat{b}_{12}) \cdot \hat{b}_{13} \, \mathrm{d}x_{21}$$

$$- \int_0^{L_2} \rho \tilde{u}_{22} \, \mathrm{d}x_{21}[\dot{s}_3' + \dot{s}_1(L_1 + q_2') + 2s_1 s_2' - s_1^2 q_3'](\hat{b}_{22} \times \hat{b}_{12}) \cdot \hat{b}_{13}$$

$$- \int_0^{L_2} \rho(x_{21} + \tilde{u}_{21})\left[\frac{\partial^2 \tilde{u}_{22}}{\partial t^2} + (\dot{s}_1 + \dot{s}_4' + \dot{s}_5)(x_{21} + \tilde{u}_{21})\right.$$

$$\left. + 2(s_1 + s_4' + s_5)\frac{\partial \tilde{u}_{21}}{\partial t} - (s_1 + s_4' + s_5)^2 \tilde{u}_{22}\right] \mathrm{d}x_{21}$$

$$+ \int_0^{L_2} \rho \tilde{u}_{22}\left[\frac{\partial^2 \tilde{u}_{21}}{\partial t^2} - (\dot{s}_1 + \dot{s}_4' + \dot{s}_5)\tilde{u}_{22} - 2(s_1 + s_4' + s_5)\frac{\partial \tilde{u}_{22}}{\partial t}\right.$$

$$\left. - (s_1 + s_4' + s_5)^2(x_{21} + \tilde{u}_{21})\right] \mathrm{d}x_{21}. \tag{29}$$

Equations (19) and (20) are replaced with

$$0 = \frac{\partial}{\partial x_{21}}\left[EA\left(\frac{\partial \tilde{u}_{21}}{\partial x_{21}} + \frac{1}{2}\left(\frac{\partial \tilde{u}_{22}}{\partial x_{21}}\right)^2\right)\right] - \rho[\dot{s}_2' - \dot{s}_1 q_3' - 2s_1 s_3' - s_1^2(L_1 + q_2')](\hat{b}_{11} \cdot \hat{b}_{21})$$

$$- \rho[\dot{s}_3' + \dot{s}_1(L_1 + q_2') + 2s_1 s_2' - s_1^2 q_3'](\hat{b}_{12} \cdot \hat{b}_{21}) - \rho_B\left[\frac{\partial^2 \tilde{u}_{21}}{\partial t^2} - (\dot{s}_1 + \dot{s}_4' + \dot{s}_5)\tilde{u}_{22}\right.$$

$$\left. - 2(s_1 + s_4' + s_5)\frac{\partial \tilde{u}_{22}}{\partial t} - (s_1 + s_4' + s_5)^2(x_{21} + \tilde{u}_{21})\right] \tag{30}$$

and

$$0 = \frac{\partial}{\partial x_{21}}\left[EA\left(\frac{\partial \tilde{u}_{21}}{\partial x_{21}} + \tfrac{1}{2}\left(\frac{\partial \tilde{u}_{22}}{\partial x_{21}}\right)^2\right)\frac{\partial \tilde{u}_{22}}{\partial x_{21}}\right] - \frac{\partial^2}{\partial x_{21}^2}\left(EI\frac{\partial^2 \tilde{u}_{22}}{\partial x_{21}^2}\right)$$

$$- \rho[\dot{s}_2' - \dot{s}_1 q_3' - 2s_1 s_3' - s_1^2(L_1 + q_2')](\hat{b}_{11} \cdot \hat{b}_{22})$$

$$- \rho[\dot{s}_3' + \dot{s}_1(L_1 + q_2') + 2s_1 s_2' - s_1^2 q_3'](\hat{b}_{12} \cdot \hat{b}_{22})$$

$$- \rho\left[\frac{\partial^2 \tilde{u}_{22}}{\partial t^2} + (\dot{s}_1 + \dot{s}_4' + \dot{s}_5)(x_{21} + \tilde{u}_{21}) + 2(s_1 + s_4' + s_5)\frac{\partial \tilde{u}_{21}}{\partial t} - (s_1 + s_4' + s_5)^2 \tilde{u}_{22}\right]. \tag{31}$$

Equations (21), (22) and (23) are replaced with

$$EA\left(\frac{\partial \tilde{u}_{21}}{\partial x_{21}} + \frac{1}{2}\left(\frac{\partial \tilde{u}_{22}}{\partial x_{21}}\right)^2\right) = 0, \tag{32}$$

$$EA\left(\frac{\partial \tilde{u}_{21}}{\partial x_{21}} + \frac{1}{2}\left(\frac{\partial \tilde{u}_{22}}{\partial x_{21}}\right)^2\right)\frac{\partial \tilde{u}_{22}}{\partial x_{21}} - \frac{\partial}{\partial x_{21}}\left(EI\frac{\partial^2 \tilde{u}_{22}}{\partial x_{21}^2}\right) = 0, \qquad EI\frac{\partial^2 \tilde{u}_{22}}{\partial x_{21}^2} = 0, \tag{33, 34}$$

respectively. Initial conditions for q_1, q_5, s_1, s_5, $\tilde{u}_{11}$, $\tilde{u}_{12}$, $\tilde{u}_{21}$, $\tilde{u}_{22}$, $(\partial \tilde{u}_{11}/\partial t)$, $(\partial \tilde{u}_{12}/\partial t)$, $(\partial \tilde{u}_{21}/\partial t)$, and $(\partial \tilde{u}_{22}/\partial t)$ must also be specified. The kinematic differential equations for q_1 and q_5 are given in equation (3) for the ordinary generalized speeds.

2.2. CONSTRAINED MOTION

In this section the equations of motion derived above will be modified to represent the dynamics of the system in its constrained configuration. First we start with the kinematic constraint between the regular and pseudo speeds then proceed to the equations of motion. Note that Lagrange multipliers are not needed, thus these constrained equations are minimally formulated.

Consider the situation depicted in Figure 2. The co-ordinates are the same as described above with the addition of two more co-ordinates. For the overall motion, modelled by ordinary differential equations, a single co-ordinate q_9 and its speed $s_9 = \dot{q}_9$ can be used to describe the system. In addition, q_8 and its speed $s_8 = \dot{q}_8$ are introduced as fictitious co-ordinates and will be used in determining switching conditions for the motion regimes.

A vector loop can be used to describe the constraints between the co-ordinates (pseudo and regular). Using the loop implied in Figure 2 the following equations hold:

$$(L_1 + q_2')(\hat{b}_{11} \cdot \hat{n}_1) + q_3'(\hat{b}_{12} \cdot \hat{n}_1) + (L_2 + q_6')(\hat{b}_{21} \cdot \hat{n}_1) + q_7'(\hat{b}_{22} \cdot \hat{n}_1) - q_9 = 0, \quad (35)$$

$$(L_1 + q_2')(\hat{b}_{11} \cdot \hat{n}_2) + q_3'(\hat{b}_{12} \cdot \hat{n}_2) + (L_2 + q_6')(\hat{b}_{21} \cdot \hat{n}_2) + q_7'(\hat{b}_{22} \cdot \hat{n}_2) - (h + q_8) = 0, \quad (36)$$

where

$$q_6' = \tilde{u}_{21}(L_2, t) \quad \text{and} \quad q_7' = \tilde{u}_{22}(L_2, t) \quad (37)$$

and q_8 is fictitious (to be used later for determining constraint violation). These relationships can be differentiated to obtain the non-holonomic constraint conditions (linear). Solving the non-holonomic constraint conditions for s_1 and s_2 gives

$$\begin{aligned} s_1 = \{ &-[(L_2 + q_6')C_{45} - q_7'S_{45}]s_2' - [(L_2 + q_6')S_{45} + q_7'C_{45}]s_3' - (L_2 + q_6')C_{45}s_6' - q_7's_7' \\ &+[(L_2 + q_6')S_{145} - q_7'C_{145}]s_8 + [(L_2 + q_6')C_{145} - q_7'S_{145}]s_9\}/\Delta \end{aligned} \quad (38)$$

and

$$\begin{aligned} s_5 = \{ &-[(L_1 + q_2') - (L_2 + q_6')C_{45} + q_7'S_{45}]s_2' - [-q_3' - (L_2 + q_6')S_{45} - q_7'C_{45}]s_3' \\ &-[(L_1 + q_2')S_{45} - q_3'C_{45}](L_2 + q_6')s_4' + [-(L_1 + q_2')C_{45} - q_3'S_{45}]q_7's_4' \\ &-[-(L_1 + q_2')C_{45} - q_3'S_{45} - (L_2 + q_6')]s_6' - [(L_1 + q_2')S_{45} - q_3'S_{45} - q_7']s_7' \\ &-[(L_1 + q_2')S_1 + q_3'C_1 + (L_2 + q_6')S_{145} + q_7'C_{145}]s_8 \\ &+[-(L_1 + q_2')C_1 + q_3'S_1 - (L_2 + q_6')C_{145} + q_7'S_{145}]s_9\}/\Delta, \end{aligned} \quad (39)$$

where

$$s_6' = \dot{q}_6' \quad \text{and} \quad s_7' = \dot{q}_7' \quad (40)$$

and where $S_1 = \sin(q_1)$, $C_1 = \cos(q_1)$, $S_{45} = \sin(q_4' + q_5)$, $C_{45} = \cos(q_4' + q_5)$, $S_{145} = \sin(q_1 + q_4' + q_5)$, and $C_{145} = \cos(q_1 + q_4' + q_5)$. The determinant Δ is defined as

$$\Delta = -(L_1 + q_2')(L_2 + q_6')S_{45} - q_3'(L_2 + q_6')C_{45} + (L_1 + q_2')q_7'C_{45} + q_3'q_7'S_{45}. \quad (41)$$

The kinematic relationships derived for the free flight are valid provided one eliminates the dependent speeds s_1 and s_5. The non-zero partial velocities needed in the remaining calculations are (considering equations (38) and (39)):

$$\frac{\partial^{\mathcal{N}}\boldsymbol{\omega}^{B_1}}{\partial s_2'} = -[(L_2 + q_6')C_{45} - q_7'S_{45}]\hat{b}_{13}/\Delta,$$

$$\frac{\partial^{o}_{\mathcal{N}}\mathbf{v}^{b_{o2}}}{\partial s_2'} = [1 + q_3'((L_2 + q_6')C_{45} - q_7'S_{45})/\Delta]\hat{b}_{11} - (L_1 + q_2')[(L_2 + q_6')C_{45} - q_7'S_{45}]\hat{b}_{12}/\Delta,$$

$$\frac{\partial^{\mathcal{N}}\boldsymbol{\omega}^{B_2}}{\partial s_2'} = (L_1 + q_2')\hat{b}_{23}/\Delta, \qquad \frac{\partial^{\mathcal{N}}\boldsymbol{\omega}^{B_1}}{\partial s_3'} = -[(L_2 + q_6')S_{45} + q_7'C_{45}]\hat{b}_{13}/\Delta,$$

$$\frac{\partial^{o}_{\mathcal{N}}\mathbf{v}^{b_{o2}}}{\partial s_3'} = q_3'[(L_2 + q_6')S_{45} + q_7'C_{45}]\hat{b}_{11}/\Delta + [1 - (L_1 + q_2')((L_2 + q_6')S_{45} + q_7'C_{45})/\Delta]\hat{b}_{12},$$

$$\frac{\partial^{\mathcal{N}}\boldsymbol{\omega}^{B_2}}{\partial s_3'} = -[(L_2 + q_6')S_{45} + q_7'C_{45} - q_3' - (L_2 + q_6')S_{45} - q_7'C_{45}]\hat{b}_{23}/\Delta,$$

$$\frac{\partial^{\mathcal{N}}\boldsymbol{\omega}^{B_2}}{\partial s_4'} = [1 - ((L_1 + q_2')S_{45} - q_3'C_{45})(L_2 + q_6')/\Delta + ((L_1 + q_2')C_{45} - q_3'S_{45})q_7'/\Delta]\hat{b}_{23},$$

$$\frac{\partial^{\mathcal{N}}\boldsymbol{\omega}^{B_1}}{\partial s_6'} = -(L_2 + q_6')C_{45}\hat{b}_{13}/\Delta,$$

$$\frac{\partial^{o}_{\mathcal{N}}\mathbf{v}^{b_{o2}}}{\partial s_6'} = q_3'(L_2 + q_6')C_{45}\hat{b}_{11}/\Delta - (L_1 + q_2')(L_2 + q_6')C_{45}\hat{b}_{12}/\Delta,$$

$$\frac{\partial^{\mathcal{N}}\boldsymbol{\omega}^{B_2}}{\partial s_6'} = [(L_2 + q_6')(1 - C_{45}) + (L_1 + q_2')C_{45} + q_3'S_{45}]\hat{b}_{23}/\Delta,$$

$$\frac{\partial^{\mathcal{N}}\boldsymbol{\omega}^{B_1}}{\partial s_7'} = -q_7'\hat{b}_{13}/\Delta, \qquad \frac{\partial^{o}_{\mathcal{N}}\mathbf{v}^{b_{o2}}}{\partial s_7'} = q_3'q_7'\hat{b}_{11}/\Delta - q_7'(L_1 + q_2')\hat{b}_{12}/\Delta,$$

$$\frac{\partial^{\mathcal{N}}\boldsymbol{\omega}^{B_2}}{\partial s_7'} = -[(L_1 + q_2')S_{45} - q_3'C_{45}]\hat{b}_{23}/\Delta, \qquad \frac{\partial^{\mathcal{N}}\boldsymbol{\omega}^{B_1}}{\partial s_8} = [(L_2 + q_6')S_{145} + q_7'C_{145}]\hat{b}_{13}/\Delta,$$

$$\frac{\partial^{o}_{\mathcal{N}}\mathbf{v}^{b_{o2}}}{\partial s_8} = -q_3'[(L_2 + q_6')S_{145} + q_7'C_{145}]\hat{b}_{11}/\Delta + (L_1 + q_2')[(L_2 + q_6')S_{145} + q_7'C_{145}]\hat{b}_{12}/\Delta,$$

$$\frac{\partial^{\mathcal{N}}\boldsymbol{\omega}^{B_2}}{\partial s_8} = -[(L_1 + q_2')S_1 + q_3'C_1]\hat{b}_{23}/\Delta, \qquad \frac{\partial^{\mathcal{N}}\boldsymbol{\omega}^{B_1}}{\partial s_9} = [(L_2 + q_6')C_{145} - q_7'S_{145}]\hat{b}_{13}/\Delta,$$

$$\frac{\partial^{o}_{\mathcal{N}}\mathbf{v}^{b_{o2}}}{\partial s_9} = [(L_2 + q_6')C_{145} - q_7'S_{145}](-q_3'\hat{b}_{11} + (L_1 + q_2')\hat{b}_{12})/\Delta,$$

$$\frac{\partial^{\mathcal{N}}\boldsymbol{\omega}^{B_2}}{\partial s_9} = [-(L_1 + q_2')C_1 + q_3'S_1]\hat{b}_{23}/\Delta. \tag{42}$$

2.2.1. *ODE's*

The ordinary differential equation for the constrained motion is

$$0 = \frac{\partial^{o}_{\mathcal{N}}\mathbf{v}^{b_{o1}}}{\partial s_9}\cdot[\mathbf{F}_{B_1} - \mathbf{I}_{B_1}] + \frac{\partial^{\mathcal{N}}\boldsymbol{\omega}^{B_1}}{\partial s_9}\cdot[\mathbf{T}_{B_1} - \mathbf{J}_{B_1}] + \frac{\partial^{o}_{\mathcal{N}}\mathbf{v}^{b_{o2}}}{\partial s_9}\cdot[\mathbf{F}_{B_2} - \mathbf{I}_{B_2}]$$
$$+ \frac{\partial^{\mathcal{N}}\boldsymbol{\omega}^{B_2}}{\partial s_9}\cdot[\mathbf{T}_{B_2} - \mathbf{J}_{B_2}]. \tag{43}$$

Replacing the symbols with their values gives

$$0 = \frac{1}{\Delta}[(L_2 + q_6')C_{145} - q_7'S_{145}]\Bigg\{M_1 - \int_0^{L_1}\rho(x_{11} + \tilde{u}_{11})\Bigg[\frac{\partial^2\tilde{u}_{12}}{\partial t^2} + \dot{s}_1(x_{11} + \tilde{u}_{11})$$
$$+ 2s_1\frac{\partial\tilde{u}_{11}}{\partial t} - s_1^2\tilde{u}_{12}\Bigg]\mathrm{d}x_{11} + \int_0^{L_1}\rho\tilde{u}_{12}\Bigg[\frac{\partial^2\tilde{u}_{11}}{\partial t^2} - \dot{s}_1\tilde{u}_{12} - 2s_1\frac{\partial\tilde{u}_{12}}{\partial t} - s_1^2(x_{11} + \tilde{u}_{11})\Bigg]\mathrm{d}x_{11}\Bigg\}$$
$$- \frac{q_3'}{\Delta}[(L_2 + q_6')C_{145} - q_7'S_{145}]\Bigg\{-\int_0^{L_2}\rho\ \mathrm{d}x_{21}[\dot{s}_2' - \dot{s}_1q_3' - 2s_1s_3' - s_1^2(L_1 + q_2')]$$
$$- \int_0^{L_2}\rho\Bigg[\frac{\partial^2\tilde{u}_{21}}{\partial t^2} - (\dot{s}_1 + \dot{s}_4' + \dot{s}_5)\tilde{u}_{22} - 2(s_1 + s_4' + s_5)\frac{\partial\tilde{u}_{22}}{\partial t}$$
$$- (s_1 + s_4' + s_5)^2(x_{21} + \tilde{u}_{21})\Bigg](\hat{b}_{11}\cdot\hat{b}_{21})\,\mathrm{d}x_{21} - \int_0^{L_2}\rho\Bigg[\frac{\partial^2\tilde{u}_{22}}{\partial t^2} + (\dot{s}_1 + \dot{s}_4' + \dot{s}_5)(x_{21} + \tilde{u}_{21})$$
$$+ 2(s_1 + s_4' + s_5)\frac{\partial\tilde{u}_{21}}{\partial t} - (s_1 + s_4' + s_5)^2\tilde{u}_{22}\Bigg](\hat{b}_{11}\cdot\hat{b}_{22})\,\mathrm{d}x_{21}\Bigg\}$$

$$+\frac{(L_1+q_2')}{\Delta}\left[(L_2+q_6')C_{145}-q_7'S_{145}\right]\Bigg\{-\int_0^{L_2}\rho\,\mathrm{d}x_{21}[\dot{s}_3'+\dot{s}_1(L_1+q_2')+2s_1s_2'-s_1^2q_3']$$

$$-\int_0^{L_2}\rho\left[\frac{\partial^2\tilde{u}_{21}}{\partial t^2}-(\dot{s}_1+\dot{s}_4'+\dot{s}_5)\tilde{u}_{22}-2(s_1+s_4'+s_5)\frac{\partial\tilde{u}_{22}}{\partial t}-(s_1+s_4'+s_5)^2(x_{21}+\tilde{u}_{21})\right]$$

$$\times(\hat{b}_{12}\cdot\hat{b}_{21})\,\mathrm{d}x_{21}-\int_0^{L_2}\rho\left[\frac{\partial^2\tilde{u}_{22}}{\partial t^2}+(\dot{s}_1+\dot{s}_4'+\dot{s}_5)(x_{21}+\tilde{u}_{21})+2(s_1+s_4'+s_5)\frac{\partial\tilde{u}_{21}}{\partial t}\right.$$

$$\left.-(s_1+s_4'+s_5)^2\tilde{u}_{22}\right](\hat{b}_{12}\cdot\hat{b}_{22})\,\mathrm{d}x_{21}\Bigg\}+\frac{1}{\Delta}\left[-(L_1+q_2')C_1+q_3'S_1\right]$$

$$\times\Bigg\{M_2-\int_0^{L_2}\rho(x_{21}+\tilde{u}_{21})[\dot{s}_2'-\dot{s}_1q_3'-2s_1s_3'-s_1^2(L_1+q_2')](\hat{b}_{21}\times\hat{b}_{11})\cdot\hat{b}_{13}\,\mathrm{d}x_{21}$$

$$-\int_0^{L_2}\rho\tilde{u}_{22}[\dot{s}_2'-\dot{s}_1q_3'-2s_1s_3'-s_1^2(L_1+q_2')](\hat{b}_{22}\times\hat{b}_{11})\cdot\hat{b}_{13}\,\mathrm{d}x_{21}$$

$$-\int_0^{L_2}\rho(x_{21}+\tilde{u}_{21})[\dot{s}_3'+\dot{s}_1(L_1+q_2')+2s_1s_3'-s_1^2q_3'](\hat{b}_{21}\times\hat{b}_{12})\cdot\hat{b}_{13}\,\mathrm{d}x_{21}$$

$$-\int_0^{L_2}\rho\tilde{u}_{22}\,\mathrm{d}x_{21}[\dot{s}_3'+\dot{s}_1(L_1+q_2')+2s_1s_3'-s_1^2q_3'](\hat{b}_{22}\times\hat{b}_{12})\cdot\hat{b}_{13}$$

$$-\int_0^{L_2}\rho(x_{21}+\tilde{u}_{21})\left[\frac{\partial^2\tilde{u}_{22}}{\partial t^2}+(\dot{s}_1+\dot{s}_4'+\dot{s}_5)(x_{21}+\tilde{u}_{21})+2(s_1+s_4'+s_5)\frac{\partial\tilde{u}_{21}}{\partial t}\right.$$

$$\left.-(s_1+s_4'+s_5)^2\tilde{u}_{22}\right]\mathrm{d}x_{21}+\int_0^{L_2}\rho\tilde{u}_{22}\left[\frac{\partial^2\tilde{u}_{21}}{\partial t^2}-(\dot{s}_1+\dot{s}_4'+\dot{s}_5)\tilde{u}_{22}\right.$$

$$\left.-2(s_1+s_4'+s_5)\frac{\partial\tilde{u}_{22}}{\partial t}-(s_1+s_4'+s_5)^2(x_{21}+\tilde{u}_{21})\right]\mathrm{d}x_{21}\Bigg\}. \tag{44}$$

Using equations (38) and (39), $\dot{s}_1$, s_1, $\dot{s}_5$ and s_5 can be eliminated in terms of $\dot{s}_9$ and s_9 and the pseudo-co-ordinates (taking s_8 and q_8 to be zero). The result can be set up as a differential equation in $\dot{s}_9$ and the pseudo-co-ordinates, which are determined via the field equations.

2.2.2. *PDE's and BC's*

The field equations are readily determined as before. In fact the equations are the same as before (equations (25), (26), (30) and (31) provided $\dot{s}_1$, s_1, $\dot{s}_5$ and s_5 are eliminated as described by the kinematic constraints.

The left-hand side of the boundary conditions for the constrained motion are the same as in equations (27)–(29) and (32)–(34). The right-hand sides are defined as

$$g'_{11} = \frac{\partial^o_{\mathcal{A}} \mathbf{v}^{b_{o1}}}{\partial s'_2} \cdot [\mathbf{F}_{B_1} - \mathbf{I}_{B_1}] + \frac{\partial^{\mathcal{N}} \boldsymbol{\omega}^{B_1}}{\partial s'_2} \cdot [\mathbf{T}_{B_1} - \mathbf{J}_{B_1}] + \frac{\partial^o_{\mathcal{N}} \mathbf{v}^{b_{o2}}}{\partial s'_2} \cdot [\mathbf{F}_{B_2} - \mathbf{I}_{B_2}] + \frac{\partial^{\mathcal{N}} \boldsymbol{\omega}^{B_2}}{\partial s'_2} \cdot [\mathbf{T}_{B_2} - \mathbf{J}_{B_2}],$$

$$g'_{12} = \frac{\partial^o_{\mathcal{A}} \mathbf{v}^{b_{o1}}}{\partial s'_3} \cdot [\mathbf{F}_{B_1} - \mathbf{I}_{B_2}] + \frac{\partial^{\mathcal{N}} \boldsymbol{\omega}^{B_1}}{\partial s'_3} \cdot [\mathbf{T}_{B_1} - \mathbf{J}_{B_1}] + \frac{\partial^o_{\mathcal{A}} \mathbf{v}^{b_{o2}}}{\partial s'_3} \cdot [\mathbf{F}_{B_2} - \mathbf{I}_{B_2}] + \frac{\partial^{\mathcal{N}} \boldsymbol{\omega}^{B_2}}{\partial s'_3} \cdot [\mathbf{T}_{B_2} - \mathbf{J}_{B_2}],$$

$$k'_{12} = \frac{\partial^o_{\mathcal{A}} \mathbf{v}^{b_{o1}}}{\partial s'_4} \cdot [\mathbf{F}_{B_1} - \mathbf{I}_{B_1}] + \frac{\partial^{\mathcal{N}} \boldsymbol{\omega}^{B_1}}{\partial s'_4} \cdot [\mathbf{T}_{B_1} - \mathbf{J}_{B_1}] + \frac{\partial^o_{\mathcal{A}} \mathbf{v}^{b_{o2}}}{\partial s'_4} \cdot [\mathbf{F}_{B_2} - \mathbf{I}_{B_2}] + \frac{\partial^{\mathcal{N}} \boldsymbol{\omega}^{B_2}}{\partial s'_4} \cdot [\mathbf{T}_{B_2} - \mathbf{J}_{B_2}],$$

$$g'_{21} = \frac{\partial^o_{\mathcal{A}} \mathbf{v}^{b_{o1}}}{\partial s'_6} \cdot [\mathbf{F}_{B_1} - \mathbf{I}_{B_1}] + \frac{\partial^{\mathcal{N}} \boldsymbol{\omega}^{B_1}}{\partial s'_6} \cdot [\mathbf{T}_{B_1} - \mathbf{J}_{B_1}] + \frac{\partial^o_{\mathcal{A}} \mathbf{v}^{b_{o2}}}{\partial s'_6} \cdot [\mathbf{F}_{B_2} - \mathbf{I}_{B_2}] + \frac{\partial^{\mathcal{N}} \boldsymbol{\omega}^{B_2}}{\partial s'_6} \cdot [\mathbf{T}_{B_2} - \mathbf{J}_{B_2}],$$

$$g'_{22} = \frac{\partial^o_{\mathcal{A}} \mathbf{v}^{b_{o1}}}{\partial s'_7} \cdot [\mathbf{F}_{B_1} - \mathbf{I}_{B_1}] + \frac{\partial^{\mathcal{N}} \boldsymbol{\omega}^{B_1}}{\partial s'_7} \cdot [\mathbf{T}_{B_1} - \mathbf{J}_{B_1}] + \frac{\partial^o_{\mathcal{A}} \mathbf{v}^{b_{o2}}}{\partial s'_7} \cdot [\mathbf{F}_{B_2} - \mathbf{I}_{B_2}] + \frac{\partial^{\mathcal{N}} \boldsymbol{\omega}^{B_2}}{\partial s'_7} \cdot [\mathbf{T}_{B_2} - \mathbf{J}_{B_2}]$$

and $k'_{22} = 0$. The leading index indicates which beam the term belongs to. The exact boundary conditions can be determined by replacing the terms with their definitions; the results are voluminous and will not be presented [37]. As can be seen in these equations, the pseudo-speeds are used to parameterize the configuration space of the system, the co-ordinate space which conforms explicitly to the applied kinematic constraints.

The condition for when the manipulator leaves the work surface (constraint violation) is when the force enforcing the constraint passes through zero. This is exactly when

$$\frac{\partial^o_{\mathcal{A}} \mathbf{v}^{b_{o1}}}{\partial s_8} \cdot [\mathbf{F}_{B_1} - \mathbf{I}_{B_1}] + \frac{\partial^{\mathcal{N}} \boldsymbol{\omega}^{B_1}}{\partial s_8} \cdot [\mathbf{T}_{B_1} - \mathbf{J}_{B_1}] + \frac{\partial^o_{\mathcal{N}} \mathbf{v}^{b_{o2}}}{\partial s_8} \cdot [\mathbf{F}_{B_2} - \mathbf{I}_{B_2}] + \frac{\partial^{\mathcal{N}} \boldsymbol{\omega}^{B_2}}{\partial s_8} \cdot [\mathbf{T}_{B_2} - \mathbf{J}_{B_2}] \tag{45}$$

changes sign. This relationship is where the fictitious speed s_8 is used, namely to form the partial velocities, every other occurrence of q_8 and s_8 are ignored. This relationship can also be used to model various forms of friction between the manipulator tip and work-piece.

2.3. CONTACT/IMPACT

In this section we present the algebraic equations needed to model the momentum exchange between free-flight and constrained motion.

At the instant the manipulator contacts the surface a non-holonomic constraint is instantly enforced. This fact can be used to derive the post-contact initial conditions for

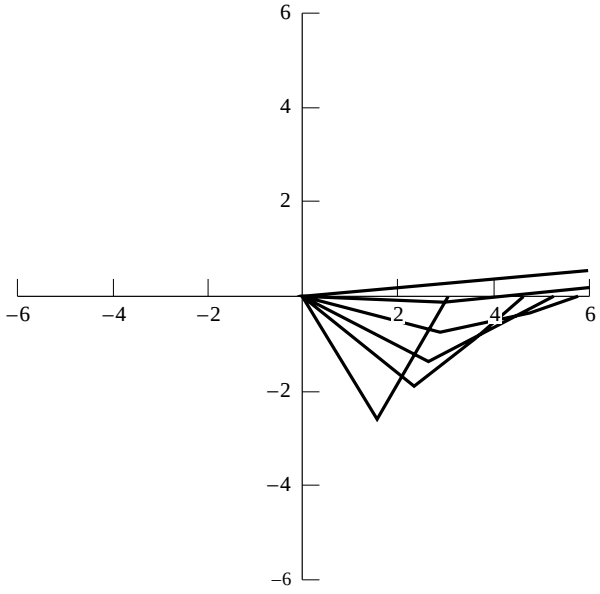

Figure 3. Animation no. 1 of a two link flexible manipulator.

the constrained motion. Previous work [35, 36] can be used for developing the algebraic momentum equations. Specifically for this problem, the initial value of s_9 is found via

$$0 = \left.\frac{\partial^o_{\mathcal{A}}\mathbf{v}^{b_{o1}}}{\partial s_9}\right|_{t_o^+} \cdot [\mathscr{F}_1 - (\mathbf{L}_1(t_o^+) - \mathbf{L}_1(t_o^-))] + \left.\frac{\partial^{\mathcal{N}}\boldsymbol{\omega}^{B_1}}{\partial s_9}\right|_{t_o^+} \cdot [\mathscr{T}_1 - (\mathbf{H}_1(t_o^+) - \mathbf{H}_1(t_o^-))]$$

$$+ \left.\frac{\partial^o_{\mathcal{A}}\mathbf{v}^{b_{o2}}}{\partial s_9}\right|_{t_o^+} \cdot [\mathscr{F}_2 - (\mathbf{L}_2(t_o^+) - \mathbf{L}_2(t_o^-))] + \left.\frac{\partial^{\mathcal{N}}\boldsymbol{\omega}^{B_2}}{\partial s_9}\right|_{t_o^+} \cdot [\mathscr{T}_2 - (\mathbf{H}_2(t_o^+) - \mathbf{H}_2(t_o^-))]. \tag{46}$$

The partial velocities are to be taken with the non-holonomic constraint applied as denoted by their evaluation at t_o^+, however, the co-ordinates in the resulting partial velocity calculations are at their pre-impact (t_o^-) values. The correct partial velocities are given in equation set (42). For the problem at hand, it is assumed that the non-constraint impulsive loadings $\mathscr{F}_1$, $\mathscr{T}_1$, $\mathscr{F}_2$ and $\mathscr{T}_2$ are zero. The linear momentum $\mathbf{L}_i(t_o^-)$ and the angular

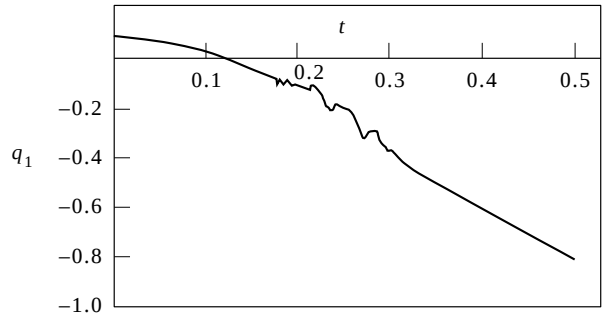

Figure 4. Co-ordinate plot case no. 1.

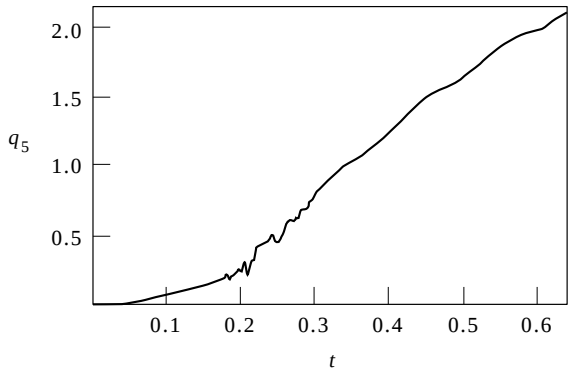

Figure 5. Co-ordinate plot case no. 1.

momentum $\mathbf{H}_1(t_o^-)$ are evaluated with speeds in the unconstrained co-ordinates. The momentum relations after contact are evaluated in the constrained co-ordinates.

The only speeds that are changed during the collision are s_6', s_7' and s_9. The other speeds are internal to the collision and are unchanged due to finite disturbance propagation speeds. The remaining two algebraic equations for determining s_6', s_7' and s_9 post-contact are

$$0 = \left.\frac{\partial_{\mathcal{N}}^{o}\mathbf{v}^{b_{o1}}}{\partial s_6'}\right|_{t_o^+} \cdot [\mathscr{F}_1 - (\mathbf{L}_1(t_o^+) - \mathbf{L}_1(t_o^-))] + \left.\frac{\partial^{\mathcal{N}}\boldsymbol{\omega}^{B_1}}{\partial s_6'}\right|_{t_o^+} \cdot [\mathscr{T}_1 - (\mathbf{H}_1(t_o^+) - \mathbf{H}_1(t_o^-))]$$
$$+ \left.\frac{\partial_{\mathcal{N}}^{o}\mathbf{v}^{b_{o2}}}{\partial s_6'}\right|_{t_o^+} \cdot [\mathscr{F}_2 - (\mathbf{L}_2(t_o^+) - \mathbf{L}_2(t_o^-))] + \left.\frac{\partial^{\mathcal{N}}\boldsymbol{\omega}^{B_2}}{\partial s_6'}\right|_{t_o^+} \cdot [\mathscr{T}_2 - (\mathbf{H}_2(t_o^+) - \mathbf{H}_2(t_o^-))] \tag{47}$$

and

$$0 = \left.\frac{\partial_{\mathcal{N}}^{o}\mathbf{v}^{b_{o1}}}{\partial s_7'}\right|_{t_o^+} \cdot [\mathscr{F}_1 - (\mathbf{L}_1(t_o^+) - \mathbf{L}_1(t_o^-))] + \left.\frac{\partial^{\mathcal{N}}\boldsymbol{\omega}^{B_1}}{\partial s_7'}\right|_{t_o^+} \cdot [\mathscr{T}_1 - (\mathbf{H}_1(t_o^+) - \mathbf{H}_1(t_o^-))]$$
$$+ \left.\frac{\partial_{\mathcal{N}}^{o}\mathbf{v}^{b_{o2}}}{\partial s_7'}\right|_{t_o^+} \cdot [\mathscr{F}_2 - (\mathbf{L}_2(t_o^+) - \mathbf{L}_2(t_o^-))] + \left.\frac{\partial^{\mathcal{N}}\boldsymbol{\omega}^{B_2}}{\partial s_7'}\right|_{t_o^+} \cdot [\mathscr{T}_2 - (\mathbf{H}_2(t_o^+) - \mathbf{H}_2(t_o^-))]. \tag{48}$$

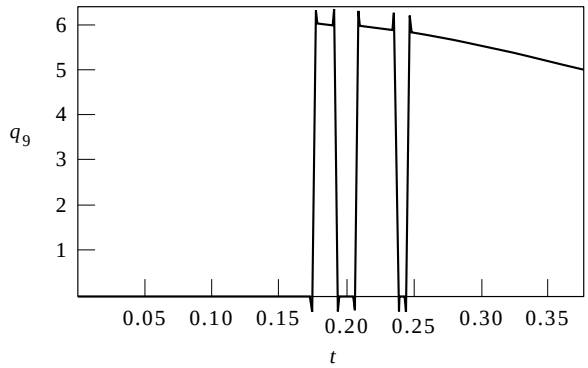

Figure 6. Co-ordinate plot case no. 1.

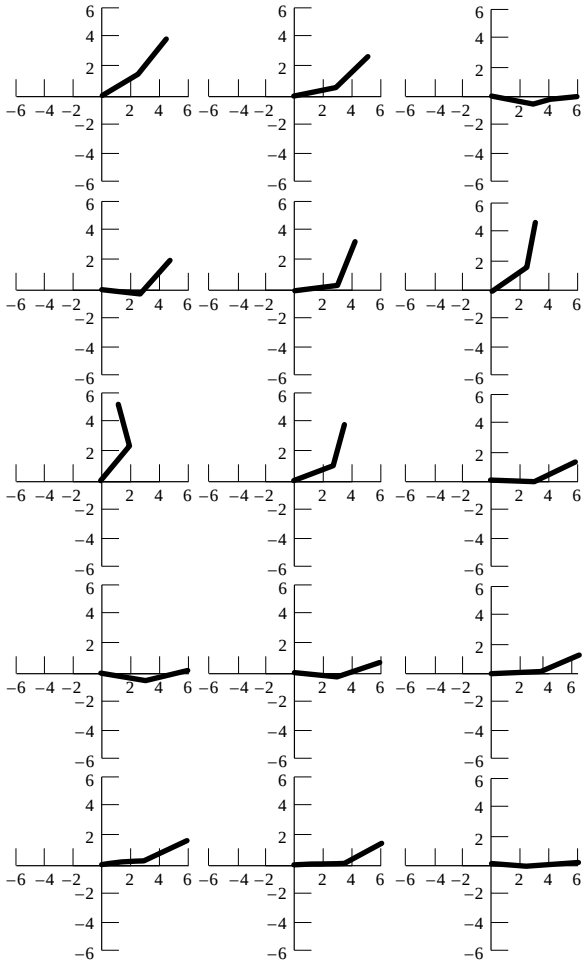

Figure 7. Animation no. 2 of a two link flexible manipulator.

The last three equations can be solved for s_6', s_7' and s_9 post-contact. The resulting s_9 is the initial s_9 for the constrained system. The pseudo-generalized speeds (s_6' and s_7') are defined in terms of the distributed co-ordinates (equations (37) and (40)) so the initial conditions for the field variables can be constructed from the previous internal velocity distribution

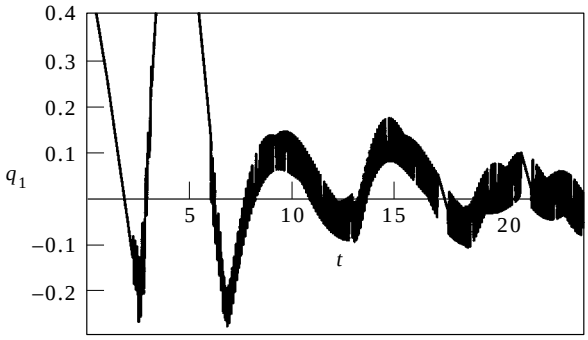

Figure 8. Co-ordinate plot case no. 2.

and the changed boundary velocity from the pseudo-speeds. The displacement field is unchanged across the instantaneous momentum exchange.

2.4. SIMULATION PREPARATION AND RESULTS

In this section the details of how the numerical model was prepared are presented. Discussed first is the field discretization proceeding to the numerical results.

The integral weak form of the partial differential equation is utilized for the numerical work. The field is assumed to have the form:

$$\tilde{u}_{e2}(x_{e1}, t) = \phi_{e1}(t)x_{e1}^2/L_{e1}^4 + \phi_{e2}(t)x_{e1}^3/L_e^4 + \phi_{e3}(t)x_{e1}^4/L_e^4, \tag{49}$$

where the elongation co-ordinates have been dropped for the sake of brevity. Structural damping proportional (γ) to the time rate of change of bending was also added to each beam's field equations. The ordinary differential equation(s) for the constrained and free motion regimes are augmented by six additional weak equations for determining the $\phi(t)$ for each continuum.*

The momentum exchange is determined by the algebraic equations shown above. For this problem, the contact/impact occurred on the boundary of the domain, therefore the post-impact velocity field is determined through the pseudo-speeds. If the momentum exchange occurs in the interior of the domain, then the algebraic field equations of momentum transfer will have to be weakened with the $\phi(t)$ discretizing the domain. This will supply the equations needed to determine the post-impact initial velocity field in terms of the $\phi(t)$.

The numerical aspects of this problem were expedited with the aid of source code generated via symbolic tools suitable for the formulation methodology [37]. To reduce the physical length of each term, judicious use of intermediate variables and the chain rule of differentiation, applied to the partial velocities, were used in formulating the minimal constrained equations of motion. The reader can become cognizant of the size of the closed-loop equation by imagining the ordinary equations of motion of the open-loop configuration in the boundary conditions for the field equations, then mentally weakening the field equations.

In order to simulate simple maneuvers a proportional control law implementing a torsional spring at each revolute joint was added. Viscous damping torques were also assumed active at each joint. Gravity was added to be able to simulate dropping the device against a surface.

Detection of contact was made by purely geometric means. When the tip of the second link was within a small distance of the surface, the time step was reduced to accurately capture the contact. Once contact was made the momentum calculations shown above were initiated and the simulation restarted in the constrained configuration. The simulation was generic enough to allow the system to be constrained initially, but not used for this work. During the constraint phase of the motion the generalized force of constrained developed above was checked to determine whether or not the system became unconstrained.

2.4.1. *Numerical results*

For the simulation, the properties were taken in consistent units to be as follows: $\rho = 1{\cdot}764$, $I = 3{\cdot}391 \times 10^{-6}$, $L_1 = 3$, $L_2 = 2$, $E = 1{\cdot}4832 \times 10^9$ and $\gamma = 0{\cdot}2$. Gravity, initial conditions, control constants, and joint damping factors were adjusted for the scenarios to follow.

* Other procedure, such as finite elements, can be used provided the formulation utilizes the constrained field equations and boundary conditions as shown.

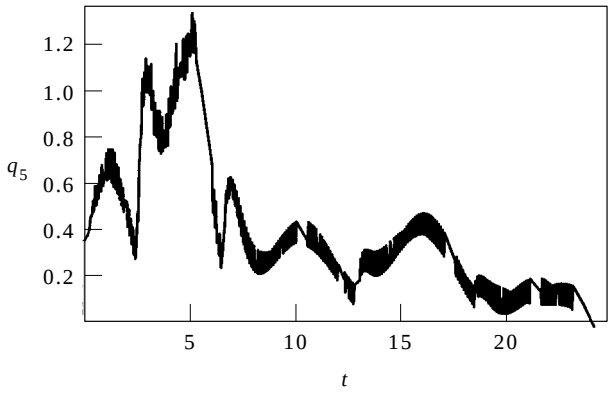

Figure 9. Co-ordinate plot case no. 2.

In the first run, the first joint was spring free; the second joint had a spring of $K_2 = 20$, zeroed at $q_5 = 0$. Both joints had damping $D = 20$. Gravity was turned on ($g = 32{\cdot}17$) and the initial condition for the joints were a few degrees positive, all others were quiescent. Figure 3 shows the animation of the motion and Figures 4, 5 and 6 show the co-ordinates q_1, q_5 and q_9, respectively. The plot for q_9 reveals the switching until the system remains constrained.

In the second run, gravity was turned off and springs $K_1 = 120$ and $K_2 = 20$ were included with set-points at the zero configuration. The joint damping was halved and the initial conditions on the angles were fairly large, with the other co-ordinates set to zero initially. Figure 7 shows the motion of the system, which lasted for 30 s, it progresses from left to right then down the page. Figures 8 and 9 show the angles. The switching occurred infrequent to the timing for simulation output so the corresponding plot for q_9 was not captured.

3. SUMMARY

In this paper an algorithm that can be used to model variable structure non-holonomic dynamics of HPMBS was presented. Demonstrated was a technique that provides closed form minimal equations of motion with minimal algebraic operations. Modelled was a planar two flexible link robot undergoing free-flight, contact/impact, and constrained motion, and the switching between these modes, which exhibits most of the dynamics that can be found in modern light-weight mechanical systems. Also provided were results for a numerical simulation that shows that experimental coefficients of restitution can be avoided by employing hybrid models, which the technique presented herein accomplishes in a systematic concise manner.

The system modelled was simple enough to be tractable by hand yet complicated enough to elucidate the technique's ability to model complex real-world systems; systems that are of variable structure such as assembly or machining robots, or systems that are free-flying such as space-born structures, or systems that are closed-loop such as automobile suspensions. Constrained systems are modelled without the use of Lagrange multipliers so that the resulting equations are minimal and the numerical difficulties associated with differential-algebraic equations are avoided.

ACKNOWLEDGEMENT

The author wishes to thank the Amarillo National Resource Center for Plutonium (ANRCP) for providing funding that allowed the completion of this work.

REFERENCES

1. K. W. Lips and R. P. Singh 1988 *Proceedings of the American Control Conference*, 587–594. Obstacles to high fidelity multibody dynamics simulation.
2. P. W. Likins 1988 *Proceedings of the Workshop on Multibody Simulation*, 10–24, JPL D-5190. Multibody dynamics: a historical perspective.
3. J. C. Simo 1988 *Proceedings of the Workshop on Multibody Simulation*, 235–296, JPL D-5190. Nonlinear dynamics of flexible structures, a geometrically exact approach.
4. L. Meirovitch 1988 *Proceedings of the IUTAM/IFAC Symposium on Dynamics of Controlled Mechanical Systems*, 37–48. Berlin: Springer-Verlag. State equations of motion for flexible bodies in terms of quasi-coordinates.
5. K. H. Low and M. Vidyasagar 1988 *Journal of Dynamic Systems, Measurement and Control* **110**, 175–181. A Lagrangian formulation of the dynamic model for flexible manipulator systems.
6. L. Petzold 1982 *SIAM Journal on Scientific and Statistical Computing* **3,** 367–384. Differential/algebraic equations are not ode's.
7. E. J. Haug and J. Yen 1989 *Proceedings of Advances in Design Automation*, 117–123, ASME. Implicit numerical integration of constrained equations of motion via generalized coordinate partitioning.
8. S. K. Ider and F. M. L. Amirouche 1989 *Journal of Dynamic Systems, Measurement and Control* **111**, 238–243. On the constraint violations in the dynamic simulations of multibody systems.
9. S. P. Timoshenko and J. N. Goodier 1970 *Theory of Elasticity*. New York: McGraw-Hill; third edition.
10. S. C. Wu and E. J. Haug 1986 *Proceedings of Advances in Design Automation*, (New York), 389–399, ASME. A substructure technique for dynamics of flexible mechanical systems with contact-impact.
11. M. G. Nasser 1992 *PhD Thesis*, *The University of Houston*, *Houston*, *TX*. Numerical methods for multibody elastic systems and contact.
12. W. J. Stronge 1994 *ASME Journal of Applied Mechanics* **61**, 605–611. Swerve during three-dimensional impact of rough bodies.
13. N. N. Kishore, A. Ghosh, S. K. Rathore and P. V. Kishore 1994 *ASME Journal of Applied Mechanics* **61**, 643–611. Finite element analysis of quasi-static problems using minimum dissipation of the energy principle.
14. J. K. Park and B. M. Kwak 1994 *ASME Journal of Applied Mechanics* **61**, 703–709. Three-dimensional frictional contact analysis using the homotopy method.
15. T. A. Laursen and V. G. Oancea 1994 *ASME Journal of Applied Mechanics* **61**, 956–963. Automation and assessment of augmented Lagrangian algorithms for frictional contact problems.
16. C.-S. Yen and E. Wu 1995 *ASME Journal of Applied Mechanics* **62**, 692–705. On the inverse problem of rectangular plates subjected to elastic impact, Parts I and II.
17. D. B. Marghitu and Y. Hurmuzlu 1995 *ASME Journal of Applied Mechanics* **62**, 725–731. Three-dimensional rigid-body collisions with multiple contact points.
18. V. Bhatt and J. Koechling 1995 *ASME Journal of Applied Mechanics* **62**, 740–746. Partitioning the parameter space according to different behaviors during three-dimensional impacts.
19. B. Wang, T. X. Yu and S. R. Reid 1995 *ASME Journal of Applied Mechanics* **62**, 887–892. Out-of-plane impact at the tip of a right-angled bent cantilever beam.
20. V. Bhatt and J. Koechling 1995 *ASME Journal of Applied Mechanics* **62**, 893–898. Three-dimensional frictional rigid-body impact.
21. J. A. Battle 1996 *ASME Journal of Applied Mechanics* **63**, 168–172. Rough balanced collisions.
22. P. Villaggio 1996 *ASME Journal of Applied Mechanics* **63**, 259–263. The rebound of an elastic sphere against a rigid wall.
23. D. Stoianovici and Y. Hurmuzlu 1996 *ASME Journal of Applied Mechanics* **63**, 307–316. A critical study of the applicability of rigid-body collision theory.
24. J. W. Gibbs 1961 *The Scientific Papers of J. Willard Gibbs*, *Volume II*: *Dynamics*, *Etc*. New York: Dover.

25. J. I. Neimark and N. A. Fufaev 1972 *Dynamics of Non-Holonomic Systems*. Providence, Rhode Island: American Mathematical Society. Translated from Russian by J. R. Barbour.
26. T. R. Kane and D. A. Levinson 1985 *Dynamics Theory and Applications*. New York: McGraw-Hill.
27. L. J. Everett and M. J. McDermott 1986 *Journal of Dynamic Systems*, *Measurement*, *and Control* **108**, 141–145. The use of vector techniques in variational problems.
28. E. A. Desloge 1987 *Journal of Guidance Control and Dynamics* **10**, 120–122. Relationship between Kane's equations and the Gibbs–Appell equations.
29. F. E. Udwadia and R. E. Kalaba 1992 *Proceedings of The Royal Society*, *London*, *Series A* **439**, 407–410. A new perspective on constrained motion.
30. H. Essén 1994 *ASME Journal of Applied Mechanics* **61**, 689–694. See discussion in Vol. 62, No. 2, pp. 552–553. On the geometry of nonholonomic dynamics.
31. J. G. Papastavridis 1994 *ASME Journal of Applied Mechanics* **61**, 453–459. On the Boltzmann–Hamel equations of motion: a vectorial treatment.
32. D. L. Mingori 1995 *ASME Journal of Applied Mechanics* **62**, 505–510. Lagrange's equations, Hamilton's equations, and Kane's equations: interrelations, energy integrals, and a variational principle.
33. J. G. Papastavridis 1995 *ASME Journal of Applied Mechanics* **62**, 924–929. On the transformation properties of the nonlinear Hamel equations.
34. A. A. Barhorst 1995 *ASME Journal of Applied Mechanics* **62**, 243–245. An alternative derivation of some new perspectives on constrained motion.
35. A. A. Barhorst and L. J. Everett 1995 *The International Journal of Nonlinear Mechanics* **30**, 1–21. Modeling hybrid parameter multiple body systems: a different approach.
36. A. A. Barhorst and L. J. Everett 1995 *Journal of Dynamic Systems*, *Measurement*, *and Control* **117**, 559–569. Contact/impact in hybrid parameter multiple body systems.
37. A. A. Barhorst 1997 *Journal of Sound and Vibration* **208,** 823–839. Symbolic equation processing utilizing vector/dyad notation.